THE JOURNAL OF BIOLOGICAL CHEMISTRY
Vol. 272, No. 21, Issue of May 23, pp. 13945–13954, 1997
Printed in U.S.A.

Replication Fork Bypass of a Pyrimidine Dimer Blocking Leading Strand DNA Synthesis*

(Received for publication, January 24, 1997, and in revised form, March 19, 1997)

Marila Cordeiro-Stone‡, Liubov S. Zaritskaya, Laura K. Price, and William K. Kaufmann

From the Department of Pathology and Laboratory Medicine, Lineberger Comprehensive Cancer Center, University of North Carolina, Chapel Hill, North Carolina 27599-7525

We constructed a double-stranded plasmid containing a single *cis,syn*-cyclobutane thymine dimer (T[c,s]T) 385 base pairs from the center of the SV40 origin of replication. This circular DNA was replicated *in vitro* by extracts from several types of human cells. The dimer was placed on the leading strand template of the first replication fork to encounter the lesion. Two-dimensional gel electrophoresis of replication intermediates documented the transient arrest of the replication fork by the dimer. Movement of the replication fork beyond the dimer was recognized by the appearance of a single fork arc in DNA sequences located between the T[c,s]T and the half-way point around the circular template (180° from the origin). Upon completion of plasmid replication, the T[c,s]T was detected by T4 endonuclease V in about one-half (46 ± 9%) of the closed circular daughter molecules. Our results demonstrate that extracts prepared from HeLa cells and SV40-transformed human fibroblasts (SV80, IDH4), including a cell line defective in nucleotide-excision repair (XPA), were competent for leading strand DNA synthesis opposite the pyrimidine dimer and replication fork bypass. In contrast, dimer bypass was severely impaired in otherwise replication-competent extracts from two different xeroderma pigmentosum variant cell lines.

Solar ultraviolet radiation is a ubiquitous environmental carcinogen responsible for 500,000 or more new cases of skin cancer in the United States each year (1, 2). Exposure of human cells to natural sunlight leads to the formation of cyclobutane pyrimidine dimers (CPDs),[1] pyrimidine(6–4)pyrimidone dimers, and their Dewar valence isomers (3). UV-induced DNA photoproducts are currently accepted as important underlying factors in skin carcinogenesis (2, 4). Studies with UVC (254 nm), which forms predominantly CPDs (70–80%) and 6–4 dimers (20–30%), have indicated that mutations and chromosomal aberrations are induced when human cells attempt to replicate the damaged DNA (5, 6). Therefore, the mechanisms whereby human cells complete the replication of template strands containing photoproducts are of considerable interest.

UVC inhibits DNA replication in diploid human fibroblast strains by a variety of mechanisms, including G_1 arrest (6) and inhibition of replicon initiation in S phase cells (7). These two checkpoint responses appear to be protective processes, providing more time for DNA repair to remove photoproducts before DNA replication. UVC also induces inhibition of DNA synthesis in active replicons (7, 8). The latter is thought to reflect, at least in part, the stalling of DNA replication forks at pyrimidine dimers (9–11), perhaps due to a reduced capacity of DNA polymerases to incorporate DNA precursors into nascent strands opposite template lesions (12–15). This inhibition, however, is not absolute, and bypass replication eventually takes place, as evidenced by the generation of replicated DNA containing photoproducts and the induction of point mutations at dipyrimidine sites. UV-induced mutations in the p53 tumor suppressor gene in non-melanoma skin cancers are characterized by a high proportion of C → T transitions (16–18). Base substitution mutations at thymines do not occur with high frequency in UV-damaged genes that are replicated at their natural chromosomal locations (19) or as part of shuttle vectors (20–22).

Previous studies have demonstrated that protein extracts from HeLa cells are capable of replicating past CPDs during *in vitro* replication of UV-damaged plasmids carrying the SV40 origin of replication (23–26). Experimental evidence in support of this conclusion was found primarily by probing for the presence of sites sensitive to nicking by the CPD-specific enzyme, T4 endonuclease V (T4 endoV), in replicated (*Dpn*I-resistant), closed circular DNA molecules (23–26). In addition, UV-induced mutagenesis at dipyrimidine sites of randomly damaged plasmids (almost exclusively C → T) presumably reflected error-prone bypass replication (trans-lesion synthesis) of CPDs (23, 24).

Bypass replication of a single dimer strategically placed on one or the other anti-parallel strand of DNA has also been examined (25, 26). Inference as to whether bypass replication occurred via leading or lagging strand synthesis was made on the basis of the location and orientation of the dimer, *vis à vis* the SV40 origin of replication, and the probability of first encounter of the CPD by one or the other of the replication forks moving in opposite direction around the circular molecule. By measuring the relative synthesis of complementary strands at restriction fragments spanning the dimer or located immediately downstream, Svoboda and Vos (25) have concluded that when the pyrimidine dimer is on the template to the leading strand the synthesis of the latter is interrupted, but the synthesis of the lagging strand continues, presumably by displacement of the replication fork beyond the lesion. In this study, we have analyzed by two-dimensional gel electrophoresis the to-

* This study was supported by U. S. Public Health Service Grant CA55065 (to M. C.-S.) and in part by Grant CA42765 (to W. K. K.). The costs of publication of this article were defrayed in part by the payment of page charges. This article must therefore be hereby marked "*advertisement*" in accordance with 18 U.S.C. Section 1734 solely to indicate this fact.

‡ To whom correspondence and reprint requests should be addressed: Dept. of Pathology and Laboratory Medicine, 522 Brinkhous-Bullitt Bldg., University of North Carolina School of Medicine, Chapel Hill, NC 27599-7525. Tel.: 919-966-1396; Fax: 919-966-5046; E-mail: uncmcs@med.unc.edu.

[1] The abbreviations used are: CPD, cyclobutane-type pyrimidine dimer; NER, nucleotide-excision repair; PRR, post-replication repair; RFI, closed circular replicative form I; RFII, nicked circular replicative form II; T4 endoV, bacteriophage T4 endonuclease V; Tag, SV40 large T antigen; T[c,s]T, *cis,syn*-cyclobutane thymine dimer; XPV, xeroderma pigmentosum variant; bp, base pair(s); kb, kilobase pair(s); SF, single fork.

pology of replicating molecules to map the displacement of DNA replication forks, in relationship to the position of the CPD, and to demonstrate directly the capability for leading strand bypass replication in human cells. Carty *et al.* (26) have recently reported that *in vitro* bypass replication of a single TT site containing either a CPD or a 6–4 dimer is poorly mutagenic.

Studies of the familial skin cancer syndrome, xeroderma pigmentosum, have revealed a form of the disease, in which a major biochemical defect in nucleotide excision repair (NER) was not detected, hence the designation of this group as variant (27–31). The defining feature of this unique xeroderma pigmentosum group is the abnormal semi-conservative replication of UV-damaged DNA (7, 8, 31–34). The high risk of cancer in sun-exposed skin (35, 36) and the enhanced sensitivity to UV-induced transformation (37, 38) and mutagenesis (39–43) support the hypothesis that xeroderma pigmentosum variant (XPV) cells have lost a gene product that participates in an essentially error-free pathway of replication of DNA containing pyrimidine dimers. Our results demonstrate that replication-competent extracts from XPV cells are deficient in the bypass of CPDs, under conditions in which other human cell extracts are capable of catalyzing this process.

EXPERIMENTAL PROCEDURES

Materials

M13mp2SV was a gift from Dr. Thomas A. Kunkel (NIEHS). Preparations of T4 endoV were provided by Dr. Isabel Mellon (University of Kentucky) and Dr. Stephen Lloyd (University of Texas Medical Branch at Galveston). The oligonucleotide containing the single T[c,s]T dimer was a gift from Dr. Aziz Sancar (University of North Carolina, Chapel Hill). Undamaged oligonucleotides were synthesized by the Nucleic Acids Core Facility of the Lineberger Comprehensive Cancer Center.

Eagle's minimal essential medium and L-glutamine were purchased from Life Technologies, Inc. Fetal bovine serum was obtained from HyClone Laboratories Inc. (Logan, UT), and gentamicin came from Elkins-Sinn Inc. (Cherry Hill, NJ). HeLa S3 cells were obtained from the Lineberger Comprehensive Cancer Center Tissue Culture Facility (University of North Carolina, Chapel Hill). Polynucleotide kinase, DNA polymerase, and DNA ligase from bacteriophage T4, as well as restriction enzymes and DNA polymerase I (Klenow fragment used to end label pUC19), were purchased from Boehringer Mannheim. The supplier of purified SV40 large T antigen was Molecular Biology Resources, Inc. (Milwaukee, WI). [α-^{32}P]dCTP (>3000 Ci/mmol) was from Amersham Life Sciences, and unlabeled nucleotides were from Pharmacia Biotech Inc. Creatine phosphate, creatine phosphokinase, and proteinase K were from Sigma.

Methods

Cell Lines, Culture Conditions, and Preparation of Cell-free Extracts—The SV40-transformed cell lines used in this study were derived from XPV fibroblasts, XP4BE (CTag, Ref. 44), and XP30RO (XP30RO/9.8, Ref. 45); XPA fibroblasts (XP12BE, GM4429, NIGMS Human Genetic Mutant Cell Repository); and other human fibroblasts (SV80, Ref. 46, and IDH4, Ref. 47). Monolayer cultures were grown in Eagle's minimal essential medium supplemented with 10% fetal bovine serum, 2 mM L-glutamine, and 50 μg/ml gentamicin in an atmosphere of 5% CO_2 at 37 °C. Extracts were prepared according to published protocols (48, 49).

Construction of M13leaSV Containing a Single T[c,s]T Dimer—The sequence 5′-GAGCTCAATTAGTCAGCTGC-3′ was introduced into the *lacZ*α sequence of M13mp2SV (50) by site-directed mutagenesis (51). This insertion created a unique *Xho*I and an additional *Pvu*II recognition site in this new construct (M13leaSV, see Fig. 1). Double-stranded, closed circular DNA molecules containing a single pyrimidine dimer were synthesized by annealing closed circular, single-stranded M13leaSV DNA (+ strand), with the oligonucleotide 3′-CTCGAG (T[c,s]T)AATCAGTCGACG-5′, previously phosphorylated at the 5′-end using T4 polynucleotide kinase. This was followed by second-strand synthesis, ligation, and purification in CsCl density gradients, according to published procedures (52). Undamaged DNA controls included RFI of M13leaSV or molecules prepared as described above but using an oligonucleotide without the dimer.

In Vitro DNA Replication—Reactions of 25 or 50 μl contained 30 mM Hepes, pH 7.8, 7 mM $MgCl_2$, 4 mM ATP, 200 μM each of the other three rNTPs, 100 μM each of the four dNTPs, 100–150 μCi/ml [α-^{32}P]dCTP, 40 mM creatine phosphate, 100 μg/ml creatine phosphokinase, 15 mM sodium phosphate, pH 7.5, 1.6 μg/ml M13leaSV DNA, 40 μg/ml SV40 large T antigen (Tag), 4 mg/ml proteins from human cell extracts (49). Reaction mixtures without Tag were used as negative controls. After incubation at 37 °C for different periods, the reactions were terminated by adding an equal volume of stop solution containing 2% SDS, 2 mg/ml proteinase K, and 50 mM EDTA. In those experiments in which the goal was to quantify specific DNA products fractionated by single dimension agarose gel electrophoresis, an identical amount of linear pUC19 DNA (end-labeled with [α-^{32}P]dCTP by *in vitro* polymerization at the *Hin*dIII cut site) was also added to each reaction. Replication products were purified by one or two extractions with an equal volume of a 1:1 (v/v) mixture of phenol and chloroform/isoamyl alcohol (24:1 v/v), followed by a final extraction with chloroform/isoamyl alcohol and then ethanol precipitation. DNA was routinely dissolved in 10 mM Tris, 1 mM EDTA, pH 7.5, and fractionated in 1% agarose gels containing 0.2 μg/ml ethidium bromide. Dried gels were analyzed with an AMBIS Image Acquisition & Analysis system (AMBIS, Inc., San Diego, CA) or exposed to a phosphor screen that was later scanned by a PhosphorImager™ (Molecular Dynamics, Sunnyvale, CA).

T4 Endonuclease V Assay—DNA replication products from either control or T[c,s]T dimer-containing templates were purified as above and incubated in the presence or absence of T4 endoV. The enzyme preparation received from Dr. Isabel Mellon (485 μg/ml; 2.7×10^{10} nicks/min/μl) was used without dilution at 1 μl per 20-μl reaction containing *in vitro* replication products in 100 mM NaCl, 10 mM EDTA, 10 mM Tris-HCl, pH 8.0, and 1 mg/ml bovine serum albumin. These reactions were incubated for 1 h at 37 °C. The T4 endoV received from Dr. Stephen Lloyd (stock solution at ~150 μg/ml) was first diluted 250 or 1000 times in reaction buffer. DNA replication products in 25 mM NaH_2PO_4, pH 6.8, 1 mM EDTA, 100 mM NaCl, 100 μg/ml bovine serum albumin were mixed with 1 μl of the diluted T4 endoV and incubated at 37 °C for 30 min. Reactions were terminated by adding one-fifth final volume of a solution containing 50% glycerol, 0.04% bromphenol blue, and 10% SDS. Subsequent to electrophoresis, the dried gels were analyzed as above.

Two-dimensional Agarose Gel Electrophoresis (53, 54)—DNA replication products were purified from 30-min reactions and digested with the indicated restriction enzyme(s). Electrophoresis was first carried out at 0.4 V/cm for approximately 68 h in 0.4% agarose gels prepared in 45 mM Tris borate, 1 mM EDTA (TBE), also containing 0.2 μg/ml ethidium bromide. Excised lanes were cast into a second gel containing 1% agarose and 0.2 μg/ml ethidium bromide in TBE. The second electrophoresis, at a 90° angle with respect to the first, was run at 1.5 V/cm for approximately 24 h. The dried gels were exposed to a phosphor screen and scanned by a PhosphorImager™.

Quantification of DNA Synthesis from AMBIS™ or Phosphor Imager™ Files—AMBIS QuantProbe Software or ImageQuaNT™ (Molecular Dynamics) was used to determine the amount of radioactivity associated with DNA by volume integration of defined regions of the scanned images. Objects were drawn with the rectangle or polygon tool to closely surround the areas of interest. In single dimensional gel electrophoresis analyses, all DNA species were included within a single object for the measurement of total DNA synthesis; specific forms (*e.g.* RFI and RFII) were quantified individually. Lane specific background was defined by a rectangle drawn under the pUC19 band. Integrated volumes (net counts) were then normalized to pUC19 recovered in each lane.

In experiments in which we incubated DNA with T4 endoV prior to gel electrophoresis, we noticed that we systematically lost a small fraction of the radiolabel incorporated at the ends of the linearized pUC19 molecules. Since this internal standard was added to each sample at the end of the *in vitro* replication reaction, the control (no enzyme addition) and treated samples contained the same ratio of total replication products to pUC19. We calculated this ratio for control samples and estimated the volume of pUC19 from the volume of total replication products for lanes containing T4 endoV. Then, this estimated volume of the internal standard was used to normalize the relative units of precursor incorporation in RFI and RFII.

Analyses of the two-dimensional gel electrophoresis images acquired with the PhosphorImager™ were done with the polygon tool and ImageQuaNT™. Only replication-intermediate arcs were quantified; volume integration was done with no background correction. The integrated volumes of bubble and fork arcs were expressed as percentages of the sum of all replicating structures detected in each image. The

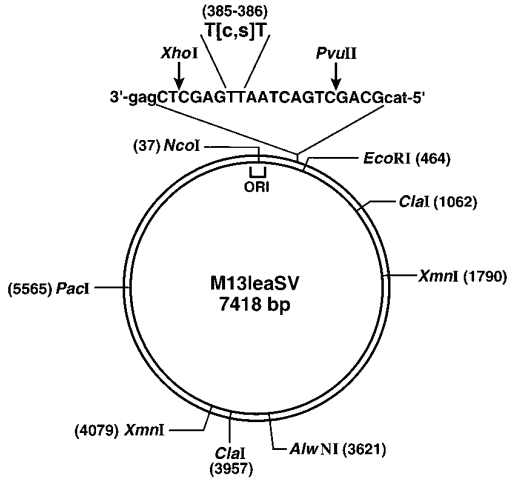

FIG. 1. **Construction of M13leaSV containing a single T[c,s]T dimer.** The diagram indicates where the dimer was placed on the template to the leading strand, relative to the SV40 origin of replication (*ORI*). M13leaSV sequence was numbered by designating as nucleotide number 1 the last G of the *Bgl*I site at the SV40 origin. The position of recognition sites for the enzymes used in this study are also noted (coordinates are given in *parentheses*). A control plasmid was constructed with an identical oligonucleotide, except for the absence of the photoproduct.

percentage distribution determined with the dimer-containing molecule was compared with that observed with the undamaged DNA.

RESULTS

Construction of M13leaSV Containing a Single T[c,s]T Dimer—Fig. 1 shows the position of the *cis,syn*-cyclobutane thymine dimer relative to the SV40 origin of replication in the double-stranded and closed circular molecule (7.4 kb) that was used as the site-specifically damaged substrate in the *in vitro* replication assays described below. These assays are dependent on Tag-directed initiation of replication at the SV40 origin and semi-conservative DNA synthesis (55) by two replication forks moving away from the origin in opposite directions (bi-directional replication). Note that in this construct, the replication fork moving from the origin toward the single *Eco*RI recognition site encounters the pyrimidine dimer (T[c,s]T) on the template to the leading strand of nascent DNA, 385 bp from the center of the SV40 origin of replication (Fig. 1).

In Vitro DNA Replication—Dimer-containing and undamaged plasmids were replicated *in vitro* with extracts from human cells. Radiolabeled products were analyzed for the degree of inhibition of RFI synthesis by the pyrimidine dimer and to determine whether the T[c,s]T was present in the newly synthesized, closed circular DNA molecules. In this experimental system, the generation of dimer-containing RFI DNA could proceed along two potentially distinct pathways (Fig. 2). If the dimer blocks one of the forks, at least momentarily (Fig. 2*A*), the other replication fork displacing in the opposite direction could complete synthesis around the circular DNA. This would generate an RFI from the undamaged strand and potentially leave the dimer in a gapped molecule. Following segregation of the daughter molecules, it is conceivable that other activities, such as gap-filling repair, could be responsible for completing synthesis across the pyrimidine dimer to form the dimer-containing RFI. Fig. 2*B* depicts the displacement of the right replication fork up to and beyond the pyrimidine dimer, thus catalyzing bypass replication, presumably by extension of the leading strand. As both pathways depicted in Fig. 2 could be operational during *in vitro* replication, it would be premature to conclude how bypass replication has taken place only from the position and orientation of the dimer in relationship to the

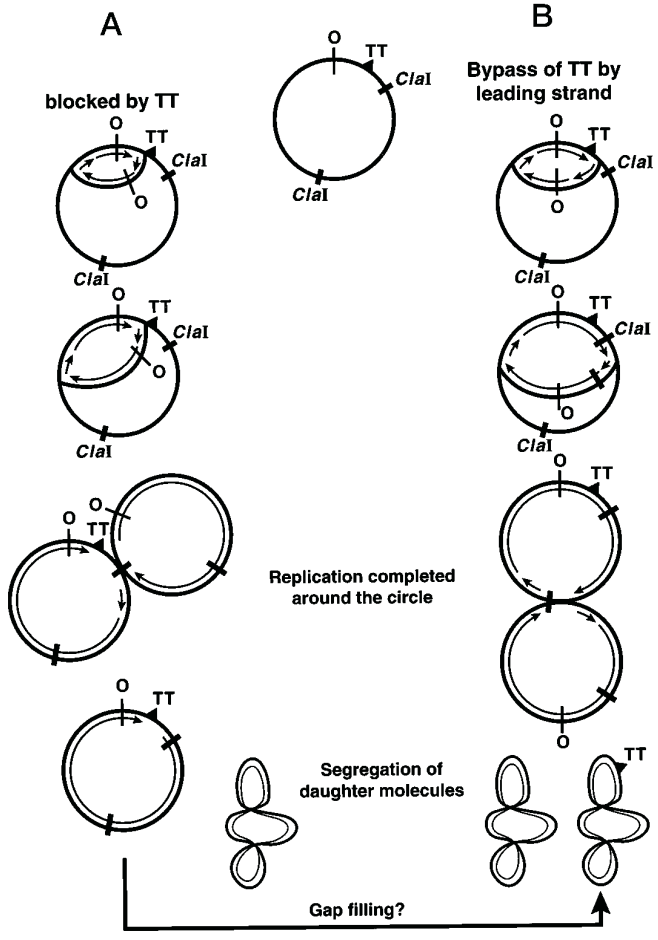

FIG. 2. **Potential effects of the T[c,s]T dimer on the *in vitro* synthesis of RFI DNA.** The dimer (*TT*) was placed on the template to the leading strand of nascent DNA synthesized by the replication fork moving to the right of the SV40 origin of replication (*O*). The diagram illustrates two scenarios as follows: *A*, complete blockage of both leading strand synthesis and displacement of the replication fork, and *B*, bypass of the TT dimer by the *right fork*. RFI DNA containing the dimer could be generated via pathway B or via pathway A if DNA synthesis by the *left fork* is followed by gap-filling.

origin of replication. Therefore, it became imperative to distinguish which pathway was more likely to be followed during replication of damaged DNA molecules *in vitro*, to investigate potential mechanisms of dimer bypass and later evaluate biological consequences of placing the lesion on the template to the leading or lagging strand of nascent DNA.

Fig. 3 illustrates the fractionation of *in vitro* replication products from reactions in which dimer-containing and control DNA were incubated with extracts from HeLa cells or XPV (CTag) fibroblasts. Results with extracts from other human fibroblasts are shown in Fig. 4. The amounts of total DNA replication products and RFI were estimated from their radioactivity (AMBIS™ or PhosphorImage™ units) after normalization to the internal standard (pUC19). Total DNA synthesis using the HeLa extract was not inhibited by the dimer. DNA synthesis on the damaged molecule averaged 98 ± 27% (mean ± S.D., $n = 20$) that on the undamaged molecule in experiments in which the incubation time varied from 1 to 6 h. In contrast, total DNA synthesis on the damaged molecule using the CTag extract was 69 ± 23% control ($n = 15$, $p < 0.01$, CTag *versus* HeLa, Student's t test). Synthesis of RFI DNA from the dimer-containing substrate was severely reduced in the CTag extract (27 ± 9%, $n = 15$) in comparison to HeLa (72 ± 22%, $n = 19$), and this difference was highly significant

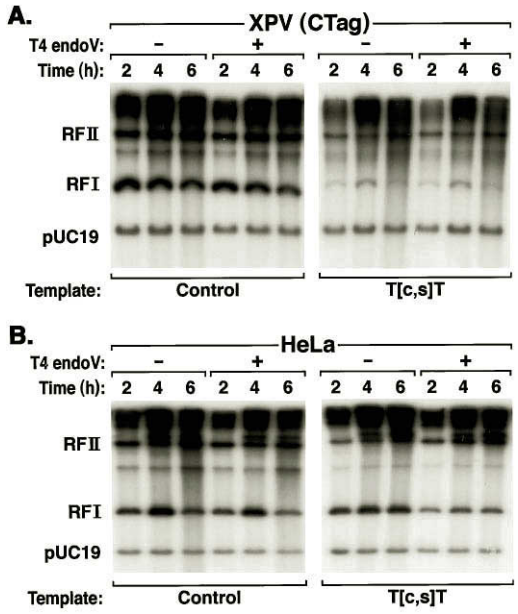

FIG. 3. **Dimer-dependent inhibition of *in vitro* DNA replication and RFI sensitivity to nicking by T4 endoV.** Extracts from XPV (CTag) and HeLa cells were incubated with control or T[c,s]T-containing template and [α-^{32}P]dCTP for 2, 4, and 6 h in the presence of Tag. As an internal standard, ^{32}P-pUC19 was added to the products of replication, which were then purified and separated by agarose gel electrophoresis. The positions of RFI, RFII, and pUC19 are indicated. For the purpose of generating this illustration, the dried gel was exposed to an x-ray film and the autoradiograph was scanned with a Pixelcraft ProImager 4000. The computer images were labeled with the color software Photoshop 3.0 in a Macintosh Power PC 8100 with system 7.0.1 and printed with a FUJIX Pictography 3000. Relative levels of RFI, as measured by the ratios of RFI/pUC19, are given below for each of the lanes in the same sequence as they appear in the figure: 3.5, 2.9, 2.6, 3.3, 2.8, 2.3, 0.56, 0.76, 0.98, 0.49, 0.74, 1.1 (*A*); and 2.9, 5.8, 3.2, 2.9, 5.8, 2.8, 3.1, 3.6, 3.9, 1.9, 2.0, 2.1 (*B*). In the same manner, values for total DNA synthesis, as reflected by the ratios of total products over pUC19, were as follows: 17, 27, 26, 15, 26, 25, 10, 16, 16, 9, 14, 15 (*A*); and 29, 45, 44, 30, 48, 47, 28, 43, 51, 28, 43, 47 (*B*).

($p < 0.005$). Thus, by two different measures of DNA synthesis, extracts from XPV cells were impaired relative to HeLa in their capacity to replicate a circular DNA molecule that contained a single pyrimidine dimer. Experiments with extracts from SV40-transformed fibroblasts (IDH4, SV80, XPA) yielded results that were comparable to those described for HeLa extracts. In the experiments illustrated in Fig. 4, for example, RFI synthesis from the T[c,s]T-containing molecules represented 86% (IDH4), 78% (SV80), and 53% (XPA) that determined with the undamaged control.

Bypass Replication of the T[c,s]T Dimer—RFI that contains a CPD is nicked by T4 endoV and converted to RFII with reduced electrophoretic mobility. By measuring the fraction of newly synthesized RFI DNA that is resistant to nicking by T4 endoV, one can calculate the fraction that carries the dimer (fraction sensitive to nicking). We determined that 0.43 ± 0.03 ($n = 5$) corresponded to the fraction of RFI DNA, produced during *in vitro* reactions (1.5 to 6 h) with the HeLa extract, that was nicked by T4 endoV (Fig. 3 and Table I). Under identical conditions, the nicked fraction of RFI synthesized from undamaged DNA by the same extract was 0.09 ± 0.08 ($n = 5$). By correcting for this background we found that 34% of the RFI DNA synthesized from the T[c,s]T-containing template by HeLa carried the dimer (theoretical maximum of 50%). Similar calculations with the data depicted in Fig. 4 revealed the presence of the dimer in 45, 52, and 54% of the RFI molecules newly synthesized by IDH4, SV80, and XPA extracts, respectively (Table I). In contrast, the small amount of RFI synthesized by

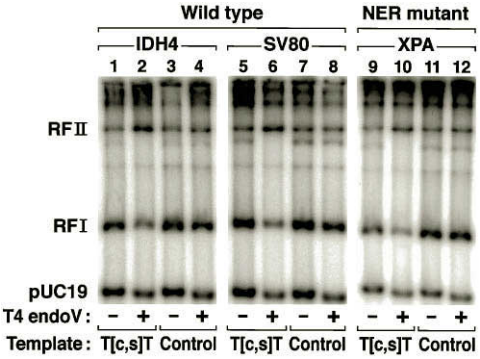

FIG. 4. **Extracts from human fibroblasts support the replication of T[c,s]T-containing plasmids, regardless of their NER capability.** Template molecules containing the T[c,s]T dimer (*lanes 1, 2, 5, 6, 9*, and *10*) or not (control in *lanes 3, 4, 7, 8, 11*, and *12*) were replicated *in vitro* during 2-h reactions with extracts from fibroblasts that are endowed with wild-type activity for NER (IDH4, *lanes 1–4*; SV80, *lanes 5–8*) or are defective in this process (XPA, NER-mutant, *lanes 9–12*). DNA was purified and incubated in the presence (+) or absence (−) of T4 endoV, as described under "Methods."

the XPV (CTag) extract from the damaged molecule (Fig. 3) demonstrated the same sensitivity to nicking by T4 endoV as the RFI products from undamaged DNA (Table I). We interpreted these results as evidence that the CTag extract was unable to complete synthesis of the template strand containing the pyrimidine dimer. Similar results were also obtained with XP30RO extracts (not shown).

We envision that the replication of T[c,s]T-containing DNA by the CTag extract followed the sequence of events illustrated on Fig. 2*A*. Absence of gap-filling repair activity could explain the T4 endoV results obtained with the XPV extract. Accordingly, if the same path is followed by all the replicating T[c,s]T-molecules in the HeLa extract, the presence of the dimer in RFI molecules would suggest that these extracts are competent to support some type of gap-filling process *in vitro*. Fig. 2*B* predicts an alternative pathway in which the complete replication of the T[c,s]T-containing DNA follows the bypass of the dimer by the right fork, the first one to encounter the lesion, thus generating one RFI containing the dimer and one RFI from the undamaged strand (50% of the RFI molecules would be sensitive to nicking by T4 endoV). Consider that in one-half of the replicating molecules the dimer is bypassed by the right fork (Fig. 2*B*), and in the other half replication is completed around the circular DNA while the right fork is still blocked at the lesion (Fig. 2*A*). Then, in the absence of gap-filling repair the expected fraction of RFI containing the dimer would be 0.33. Results of dimer-dependent nicking by T4 endoV of RFI DNA synthesized by the HeLa extract (see above) are consistent with this prediction.

Topology of Intermediates of DNA Replication—To determine whether the synthesis of RFI DNA carrying the T[c,s]T dimer was the product of elongation of the leading strand and replication fork bypass, or gap-filling repair, we analyzed the topology of intermediates of DNA replication by two-dimensional gel electrophoresis (53, 54) and deduced the position of the replication forks relative to the pyrimidine dimer. The probability of the unblocked fork moving around the circular molecule and rescuing the blocked fork (Fig. 2*A*) was reduced by decreasing to 30 min the incubation time for the *in vitro* replication reactions. After this short incubation, the labeling associated with RFI DNA represented only 3–5% of the total Tag-dependent products of replication (results not shown), when undamaged molecules were replicated with HeLa or CTag extracts, and even less when HeLa (~2%) or CTag (none detected) extracts were used to replicate the damaged plasmid. Data illustrated

TABLE I

T4 endonuclease V-sensitive sites in RFI DNA synthesized in vitro

DNA products of *in vitro* replication were incubated with T4 endoV to determine the fraction of RFI molecules containing the T[c,s]T (dimer-dependent nicked fraction). The amount of RFI remaining after treatment (normalized to the internal standard) was divided by the amount of RFI in identical samples incubated in the absence of the enzyme. This ratio (T4 endonuclease V-resistant fraction) was subtracted from 1 to determine the nicked fraction. The dimer-dependent fraction was the difference between the nicked fractions in T[c,s]T-containing and control DNA.

Extract source	Incubation time	Nicked fraction		
		Control molecule	T[c,s]T-molecule	Dimer-dependent
	h			
A. HeLa	1.5	0.17	0.43	0.26
	2.0	0.00	0.39	0.39
	3.0	0.16	0.44	0.28
	4.0	0.00	0.44	0.44
	6.0	0.13	0.46	0.33
	Mean ± SD,	0.09 ± 0.08	0.43 ± 0.03	0.34 ± 0.07
B. IDH4	2.0	0.10	0.55	0.45
C. SV80	2.0	0.00	0.52	0.52
D. XPA	2.0	0.00	0.54	0.54
E. XPV (CTag)	1.5	0.03	0.13	0.10
	2.0	0.06	0.13	0.07
	3.0	0.15	0.14	−0.01
	4.0	0.03	0.03	0.00
	6.0	0.12	0.00	−0.12
	Mean ± SD,	0.08 ± 0.05	0.09 ± 0.07	0.01 ± 0.08

in Fig. 5 confirmed that during the 30-min incubation there was insufficient time for the unblocked fork to approach the pyrimidine dimer from the opposite direction. Upon digestion with *Alw*NI, a restriction enzyme with a single recognition site ~180° from the SV40 origin (Fig. 1), the replication intermediates behaved in the two-dimensional gels as a family of molecules containing replication bubbles of various sizes. Note that the extension of the bubble arc was slightly reduced in the samples containing the damaged template (Fig. 5, *B* and *D*), as compared with the undamaged control (Fig. 5, *A* and *C*). Most remarkable, however, was the absence of a double fork arc in Fig. 5, *B* and *D*. If the replication fork expanding away from the dimer had been displaced beyond the *Alw*NI site (Fig. 1), and the other fork was stalled at the CPD (Fig. 2*A*), enzyme digestion of these partially replicated molecules would occur within the replication bubble and generate molecules containing a large fork at one end and a smaller one at the other. If these double fork molecules were present, they would generate a distinct arc (Fig. 5, *E* and *F*), separable from that displayed by the bubble-containing molecules (53, 54), as illustrated in Fig. 5, *G* and *H*.

The progression of the replication fork traveling up to and beyond the pyrimidine dimer on the right side was monitored by digesting the replicating molecules with *Cla*I. This restriction enzyme cuts M13leaSV at two different positions, 677 bp beyond the T[c,s]T dimer and about 180° from the SV40 origin of replication (Figs. 1 and 2). Thus, *Cla*I digestion of this circular DNA molecule produced fragments of 4.5- and 2.9-kb in length, with the SV40 origin of replication located off-center in the 4.5-kb fragment (Fig. 6*D*). Accordingly, two-dimensional gel electrophoresis of products from the undamaged substrate revealed two families of intermediates of replication, both associated with the 4.5-kb fragment, but with two distinct topologies (compare diagrams in Figs. 2 and 6*D*). One family migrated in the two-dimensional gels as a bubble arc because the right fork had not yet reached the *Cla*I site closest to the SV40 origin. Subsequent to the replication of this *Cla*I site, the 4.5-kb replicating fragments migrated along a single fork (SF) arc. This led also to the simultaneous appearance of a distinct SF arc in association with the 2.9-kb fragment (Fig. 6, *B*, *E*, and *H*). Note that the amount of radioactivity associated with each one of the replication arcs is a function of the number of replicating molecules, the length of the fragment, and how much of it has been replicated (*i.e.* incorporated radiolabeled DNA precursors). We detected equivalent distributions of radioactivity in these three arcs of replicative structures when undamaged molecules were replicated with extracts from HeLa (Fig. 6*B*), IDH4 (Fig. 6*E*), CTag (Fig. 6*H*), or XPA (Fig. 7*A*), suggesting that displacement rates of replication forks were very similar in replication-competent extracts from these four types of cells. This finding supports the conclusion that CTag extracts do not lack any of the basic components of the enzymatic machinery that catalyzes the semi-conservative replication of undamaged DNA.

Strikingly different results were obtained when the T[c,s]T-containing DNA was replicated *in vitro*. Fig. 6, *C* and *F*, clearly shows SF arcs in association with the 2.9-kb fragment from DNA replicated with extracts from HeLa or the SV40-transformed normal fibroblast (IDH4), albeit less intense than those observed with the undamaged template in Fig. 6, *B* and *E*, respectively. However, no SF arc was detected in association with the 2.9-kb fragment when the damaged molecule was replicated by extracts from XPV cells (*CTag*, Fig. 6*I*). This result also demonstrated that our preparations of T[c,s]T-containing DNA were devoid of detectable contamination with undamaged molecules. Furthermore, data from experiments in the absence of Tag (Fig. 6, *A* and *G*) indicate that the radioactivity detected in the 2.9-kb linear fragment (Fig. 6*I*) was not incorporated via DNA replication. Instead, it appears to reflect random incorporation of [^{32}P]dCMP, as evidenced by the labeling of the two *Cla*I linear fragments in the absence of any arcs of replicating intermediates (Fig. 6, *A* and *G*). Results identical to those displayed in Fig. 6, *H* and *I*, were obtained with extracts from SV3CRL9.7, another immortalized clone of XP4BE (44), and XP30RO/9.8, a cell line from a different XPV patient (45). Thus, bypass replication of the pyrimidine dimer by extracts from three different XPV cell lines (two independent patients) was undetectable, under the experimental condi-

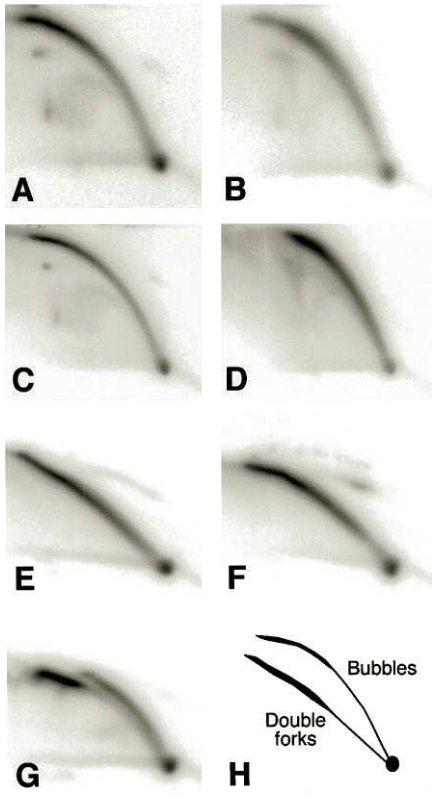

FIG. 5. **Two-dimensional gel electrophoresis of intermediates of *in vitro* DNA replication after digestion with different restriction enzymes.** M13leaSV contains a single recognition site for *Alw*NI at approximately 180° from the center of the SV40 origin (Fig. 1). Control molecules (*A, C,* and *E–G*) or T[c,s]T-containing molecules (*B* and *D*) were incubated for 30 min with extracts from HeLa (*A* and *B*) or CTag (*C–G*). The purified DNA was digested with *Alw*NI (*A–D*), *Nco*I (*E*), *Eco*RI (*F*), or *Pac*I (*G*) and fractionated by two-dimensional electrophoresis, as described under "Methods." Each one of these enzymes has a single restriction site in M13leaSV (Fig. 1). Thus, the digestion of replicating M13leaSV molecules with these enzymes generates symmetric bubbles (*Alw*NI), symmetric double forks (*Nco*I), or asymmetric double forks (*Eco*RI, *Pac*I). In a number of replicating molecules the left fork had not yet reached the *Pac*I site; therefore, in *G* one can clearly identify the lower part of a bubble arc, as well as the top part of the asymmetric double fork arc. Illustrations were prepared directly from converted image files. In *H* we show schematically a comparison of the relative positions of symmetric bubble (*A*) and double fork (*E*) arcs generated from the same population of replication intermediates.

tions used in this study. On the other hand, extracts from NER-deficient cells (XPA) displayed capability for bypass replication of CPDs by the T4 endoV assay (Fig. 4) and the two-dimensional gel electrophoretic analysis (Fig. 7).

The results with XPV extracts also confirmed that in these experiments the left fork had insufficient time to proceed around the plasmid, invade the the 2.9-kb fragment, and create SF-containing molecules. Thus, the simultaneous detection of the two SF arcs in association with the 4.5- and 2.9-kb fragments signals the displacement of the right fork beyond the nearby *Cla*I site and, by inference, the bypass of the T[c,s]T dimer (Fig. 2*B*). Judging from the percentage of the total radioactivity that was found associated with these fork arcs, bypass of the pyrimidine dimer during the 30-min incubation occurred in approximately 46, 61, or 72% of the damaged molecules that were replicated by HeLa, IDH4, or XPA extracts, respectively. Results from five independent experiments with these three bypass-proficient extracts yielded an average of 63 ± 14%. These results now clearly demonstrate that newly replicated RFI DNA containing the T[c,s]T dimer (detected by T4 endoV) was the product of dimer bypass by the replication fork that first encountered the lesion (Fig. 2*B*). Bypass replication under our experimental conditions (≤30 min) also appears to require the participation of a factor that is absent or defective in extracts from XPV cells.

Further inspection of Figs. 6, *C*, *F*, and *I*, and 7*B* also reveals the presence of labeled structures of higher molecular weights than those discussed above. Their position in the two-dimensional gels suggests a relationship with end-to-end molecules of 7.4-kb in size, *i.e.* replicating molecules that were not digested by *Cla*I in all sites (Fig. 2). This incomplete digestion appeared to be restricted to the replicating DNA (radiolabeled) because ethidium bromide fluorescence of the gels prior to dehydration allowed for the visualization of only the expected fragments of plasmid DNA. The amount of radioactivity associated with the partially restricted DNA was even higher when replication intermediates were co-digested with *Alw*NI and *Eco*RI (Fig. 8, *B* and *C*) but not as conspicuous when *Xmn*I was used (Fig. 8, *E* and *F*). We suspect that the secondary structure of DNA around the blocked replication forks was not compatible with complete cutting by *Eco*RI, *Cla*I, or other restriction enzymes with recognition sites within 1.4 kb of the 5′ side of the dimer. This might have resulted from the proposed uncoupling of leading and lagging strand synthesis in replication forks blocked by a pyrimidine dimer (25), or an *N*-2-acetylaminofluorene adduct (56, 57), thus generating long stretches of single-stranded DNA beyond the template lesion. These results would be consistent with the model depicted in Fig. 9*A*. Daughter-strand gaps of 800–1250 nucleotides have been detected in newly replicated DNA following UV irradiation of human cells (58, 59). This model is supported by the results of two-dimensional gel electrophoretic analyses showing predicted increases in the amount of replication intermediates in bubble arcs (Fig. 9*C*) and decreases to control levels of the amount of replication intermediates trapped in the 7.4-kb replication arc (Fig. 9*D*), as the restriction digestion site is moved further downstream from the pyrimidine dimer. The faint arc seen in Figs. 6*I* and 8*, C* and *F*, at about the same position as the SF arc rising from the large restriction fragment, could be due to breakage of the long single-stranded DNA regions in the anomalous 7.4-kb replication intermediate.

DISCUSSION

The process of replication of DNA containing obstructive lesions is poorly understood. Consequently, we lack clear and precise terms to describe it. Structural alterations in template DNA can be overcome during semi-conservative DNA synthesis to generate fully replicated molecules still containing the primary lesion. This process is commonly denoted in the literature as post-replication repair (PRR). Bypass replication is another term that has been used in its broader sense as a synonym for PRR or more narrowly to evoke a sub-set of proposed PRR pathways (60). Neither of these two terms, however, conveys information on how the replication machinery responds to lesions on template DNA or the mechanisms involved in the replication of the damaged substrate.

We prefer to use the term bypass replication in its broad sense as synonymous of PRR and have adopted the term replication fork bypass to connote the movement of the replication machinery through and beyond the damaged site in template DNA. In this study we have focused primarily on the effect of a pyrimidine dimer (placed on the template for the leading strand) on replication fork displacement and generation of completely replicated molecules. According to the model proposed by Meneghini and Hanawalt (11), an UV-induced pyrimidine dimer in the template for the leading strand (growing in the 5′ → 3′ direction) temporarily blocks DNA synthesis and fork movement. If the dimer is instead in the template for the

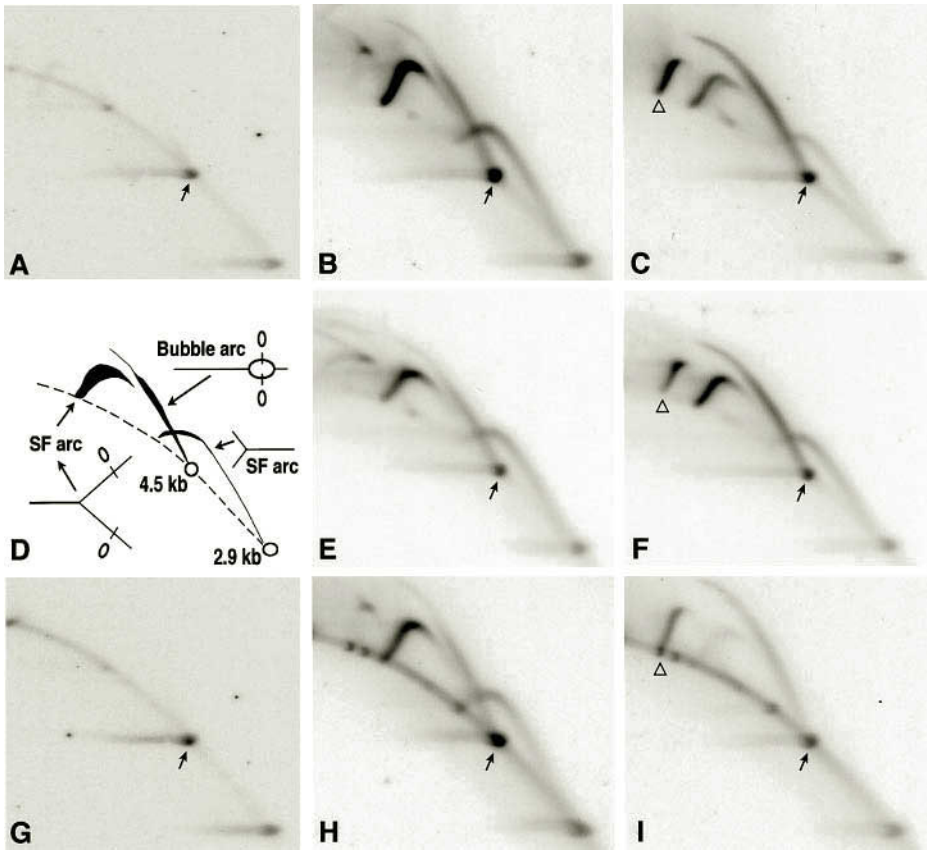

FIG. 6. **Two-dimensional agarose gel electrophoresis analyses of replication intermediates digested with *Cla*I.** Extracts from HeLa (*A–C*), IDH4 (*E* and *F*), or CTag (*G–I*), in the presence (*B*, *C*, *E*, *F, H*, and *I*) or absence (*A* and *G*) of Tag, were incubated for 30 min with control DNA (*A*, *B, E*, *G*, and *H*) or DNA carrying the single T[c,s]T dimer (*C*, *F*, and *I*). The purified DNA was digested with *Cla*I and separated by two-dimensional gel electrophoresis. The position of the 4.5-kb linear fragment is indicated in all panels with an *arrow*; the arcs of replicating intermediates associated with the 4.5- and 2.9-kb fragments are identified in *D*. The arcs identified by the *open triangles* in *C*, *F*, and *I* are discussed in the text.

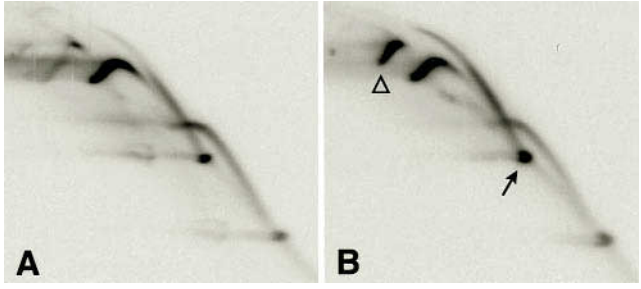

FIG. 7. **Extract of NER-deficient cells displays capability for replication fork bypass of a pyrimidine dimer.** Control molecules (*A*) or T[c,s]T-containing molecules (*B*) were replicated *in vitro* with an extract of SV40-transformed XPA cells, under the conditions described under "Methods." The purified DNA was restricted with *Cla*I and analyzed as described in Fig. 6.

lagging strand (growing discontinuously in the $3' \rightarrow 5'$ direction), a long-lived daughter-strand gap is generated following the interruption of a single Okazaki fragment (61). The lagging strand gaps are eventually filled in by mechanisms that could be operating away from the replication fork. The nature of the protein complexes that catalyze this process is unclear at this time. Gap-filling repair via homologous recombination has been difficult to prove or to discount as an important PRR mechanism in human cells (60). Alternatively, the gaps are closed in by *de novo* synthesis (58) with factors that may or may not be regular components of the enzymatic machinery associated with replication forks.

The experiments reported here were planned with two goals in mind. We wished to establish whether bypass replication of pyrimidine dimers in human cells occurred concurrently with replication fork movement beyond the lesion (Fig. 2*B*). We were also interested in determining whether PRR-defective XPV cells are deficient in bypass replication of CPDs. After creating an immortalized XPV cell line (CTag) and preparing competent extracts for *in vitro* replication (44), we determined that the synthesis of RFI DNA (Fig. 3) from molecules containing a single T[c,s]T dimer (Fig. 1) was inhibited by 73% when XPV extracts were used or 2.6-fold more strongly than when HeLa extracts replicated the same plasmid. Furthermore, the RFI molecules synthesized by XPV extracts were devoid of T4 endoV-sensitive sites (Fig. 3 and Table I), suggesting that XPV extracts did not support detectable levels of CPD bypass replication. These results were in sharp contrast to those obtained with extracts from PRR-proficient cells (Figs. 3 and 4).

Two-dimensional gel electrophoresis of intermediates of DNA replication has proven to be a very powerful technique for mapping and characterizing origins of DNA replication (53, 54, 62, 63). Because the behavior in two-dimensional gels of DNA molecules containing branches and bubbles has been characterized, this technique is well-suited for determining the effect of a site-specific CPD on the progression of replication forks along circular duplex DNA molecules. The results depicted in Figs. 5–8 show clearly that the patterns of replication intermediates observed by two-dimensional gel analyses were consistent with that expected from the map in Fig. 1. For instance, bubble arcs were observed only in association with restriction fragments containing the SV40 origin of replication, whereas distal fragments displayed the presence of single fork arcs. Kinetic experiments and two-dimensional gel analysis of replication products digested with *Alw*NI (Fig. 5) established that 30 min was insufficient time for the left replication fork to travel around the circular DNA and approach the dimer from downstream sequences. Figs. 6–8 show single fork arcs that herald the replication of restriction enzyme recognition sites located further away from the SV40 origin of replication than the pyrimidine dimer (Fig. 1). These results constitute very strong evidence that the right fork progressed beyond the dimer, thus demonstrating replication fork bypass.

HeLa extracts and those prepared from SV40-transformed

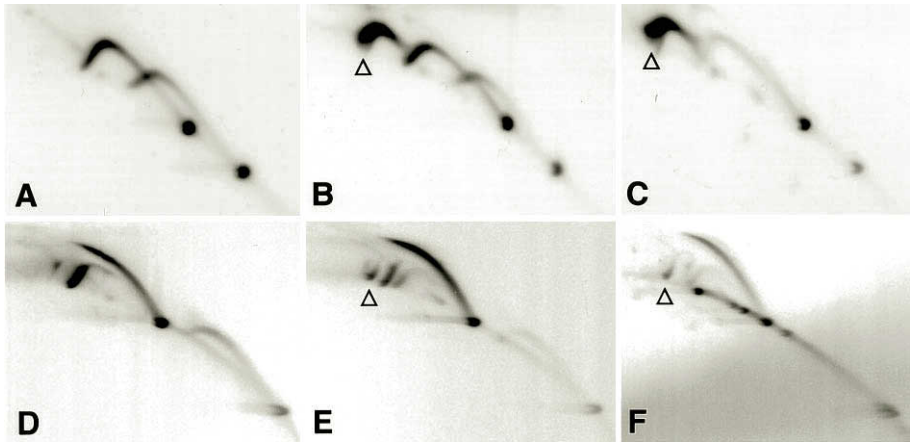

FIG. 8. **Probing the structure of replication intermediates with other restriction endonucleases.** Products of *in vitro* DNA replication of control molecules (*A* and *D*) or T[c,s]T-containing molecules (*B*, *C*, *E*, and *F*) with extracts from HeLa (*A*, *B*, *D*, and *E*) or CTag (*C* and *F*) were digested with both *Eco*RI and *Alw*NI (*A–C*) or with *Xmn*I (*D–F*) and analyzed by two-dimensional gel electrophoresis. Results with HeLa or CTag extracts were indistinguishable when control molecules were used. Thus, the CTag controls were omitted from the illustration. The *triangles* point to the 7.4-kb replication intermediate arc (see text).

human fibroblasts (IDH4, SV80) were equally competent for bypass replication of pyrimidine dimers (Figs. 6 and 8). This proficiency was not related to the presence or absence of NER activity. Extracts from XPA cells were competent for replication fork bypass (Fig. 7), and the dimer was found in molecules replicated by extracts from non-XPV cells (Figs. 3 and 4; Table I). Therefore, NER did not precede replication fork bypass. Results with immortalized human fibroblasts demonstrated that the capability for bypass replication detected in HeLa extracts (this report; Refs. 23–26) was not peculiar to these malignant cells but instead a characteristic of the replication of UV-damaged DNA in humans. The lack of bypass replication in XPV extracts was not related to the immortalization of the XPV cells by Tag, as IDH4, SV80, and XPA cells were immortalized with the same oncoprotein. Finally, detection of replication fork movement beyond the T[c,s]T dimer by two-dimensional gel electrophoresis and quantification of the percentage of replicating molecules (63 ± 14%) in which this bypass was accomplished within the first 30 min of *in vitro* incubation demonstrated for the first time that bypass replication occurs concomitantly with replication fork bypass, presumably by a mechanism that permits the elongation of the leading strand blocked by the dimer (see below).

In the human cell extracts used in this study, the DNA replication machinery was arrested by the T[c,s]T dimer found in the template for the leading strand. This arrest was temporary in molecules replicated by extracts proficient in bypass replication, and it was followed by movement of the replication fork beyond the pyrimidine dimer. It was the appearance of an anomalous arc of replicating structures of higher molecular weight (1 × = 7.4 kb) than those expected to be associated with restriction fragments (Figs. 6–8) that suggested to us that the presence of the T[c,s]T dimer in the template for the leading strand was affecting the progression of the replication fork in a very peculiar way. Until recently, our working model of an active replication fork depicted the leading strand synthesis spearheading the opening of the replication fork and the discontinuous synthesis of the complementary strand "lagging" behind. Thus, we expected that blocking of leading strand synthesis by the T[c,s]T dimer would automatically halt the displacement of the replication fork. Consequently, we predicted that after digestion of products of *in vitro* replication on the damaged substrate with *Eco*RI (together with *Alw*NI), *Cla*I, or *Xmn*I, a larger fraction of the radioactivity associated with replication intermediates would be found in the bubble arc, in comparison to undamaged controls. This prediction was only partially fulfilled by the results shown in Fig. 9*C*. The restriction fragment containing the SV40 origin of replication displayed a more prominent bubble arc as the restriction enzyme digestion site was moved further away from the origin in the undamaged substrate molecule. Likewise, when the T[c,s]T-containing substrate was replicated by extracts deficient or proficient in bypass replication, the relative representation of the bubble arc was increased upon digestion with *Cla*I or *Xmn*I. We were surprised, however, that when products of replication of the T[c,s]T-containing plasmid were restricted with *Eco*RI, the bubble arc was barely detectable (Fig. 9*C*) and instead a strong radioactive signal was found in association with the 7.4-kb replication arc (Fig. 9*D*). Since the 1 × size of the molecules forming this 7.4-kb arc was exactly the genome size of M13leaSV, it was likely that in a fraction of replication intermediates only one of the two *Eco*RI sites within the replication bubble had been cut (Fig. 9*B*). Furthermore, the shape of the arc strongly suggested branched molecules instead of bubble-containing molecules (Fig. 5). These observations, together with those in the literature suggesting that lagging strand synthesis becomes uncoupled from leading strand synthesis upon encountering a DNA lesion in the template for the leading strand (25, 56, 57), are best explained by the model illustrated in Fig. 9*B*. The salient characteristics of this model are as follows: (i) the fork structure created by the gradual melting of the duplex DNA, presumably through the activities of DNA helicases and topoisomerases, is followed closely behind by the priming and elongation of the next Okazaki fragment of the lagging strand; (ii) elongation of the leading strand occurs simultaneously, but its 3′ growing end is found at sequences preceding those already initiated in the lagging strand (64); (iii) upon blocking of leading strand elongation by the dimer, priming and synthesis of the lagging strand continues to open up the fork before its movement is stalled. Consequently, a stretch of template for the leading strand is left as single-stranded DNA that cannot be digested by restriction endonucleases. Cutting the replicating molecules at ~180° from the origin and on the lagging strand side of the extended replication bubble would generate branched molecules expected to migrate in the two-dimensional gels as the 7.4-kb replication arc. The results depicted in Fig. 9*D* seem to suggest that the single-stranded template DNA at the replication fork might extend ~700–1400 nucleotides beyond the dimer. These lower and upper limits are suggested by the still large radioactive

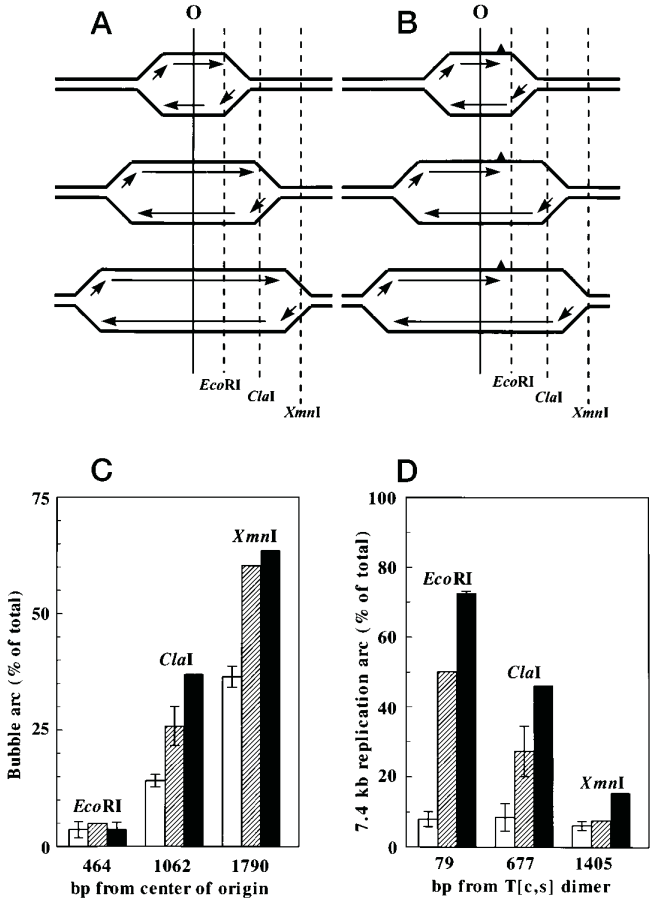

FIG. 9. **Interpretation of the structure of replicating DNA from results of two-dimensional gel electrophoresis analyses.** In the experimental system used in this study, the SV40 origin directs the initiation of DNA replication and the assembly of two replication forks that propagate in opposite directions around the circular duplex DNA. *A* depicts the progressive enlargement of the replication bubble in undamaged molecules. *B* illustrates the proposed effect of the pyrimidine dimer in blocking the elongation of the leading strand but allowing the replication fork to displace forward (uncoupling) and catalyze the synthesis of the lagging strand. It is envisioned that the rate of displacement of the right fork in the presence of the lesion is lower than in the control molecules, decreasing further as the distance from the blocked leading strand increases, until the fork is arrested in proximity to the *Xmn*I recognition site. *C* and *D* depict the percentage of the total radioactivity in replicating structures that are associated with bubbles (*C*) or with the larger 7.4-kb replication intermediate (*D*). The latter is thought to be generated by the restriction enzymes cutting the newly synthesized lagging strand but not cutting the single-stranded template generated by the blockage of elongation of the nascent leading strand. The *bars* in *C* and *D* represent average results with all extracts on control plasmids (*open*) and bypass-competent extracts (*hatched*) or bypass-deficient extracts (*filled*) on the damaged plasmid.

signal associated with the 7.4-kb intermediate in replication products digested with *Cla*I, which dropped to control levels (especially in bypass-proficient cells) when DNA was digested with *Xmn*I (Fig. 9*D*). These interpretations are also strongly supported by results of the size and frequency of daughter-strand gaps in irradiated human cells, as measured by the estimated target size of S_1 nuclease-sensitive sequences in DNA replicated after UV (59). It was found that 65% of these daughter-stranded gaps (single-stranded template regions) corresponded to stretches of 1250 nucleotides and 35% to stretches of 150 nucleotides. The smaller class is thought to represent gaps formed in the lagging strand by the interruption of an Okazaki fragment (59, 61). We now submit that the larger class represents single-stranded regions of DNA template created by blocking of leading strand synthesis by the dimer and uncoupling of lagging strand synthesis (25, 56, 57).

Having discussed the evidence for replication fork bypass of pyrimidine dimers in humans and the implication that the extension of the blocked leading strand is catalyzed by enzyme activities associated with the replication fork, it remains to be determined by which mechanism this occurs. Two formal possibilities can be envisioned at this time, mainly trans-lesion synthesis or strand switching. O'Day *et al*. (14) have shown that proliferating cell nuclear antigen facilitates trans-dimer bypass by DNA polymerase δ on a primed single-stranded oligonucleotide. More recently, DNA polymerase ξ has been discovered in yeast and shown by *in vitro* assays to catalyze trans-dimer synthesis very efficiently (15). It is assumed that these polymerases and accessory proteins operating as components of active DNA replication complexes should be capable of trans-dimer synthesis *in vitro* and *in vivo*. In this regard, it is noteworthy that a mutation in proliferating cell nuclear antigen has been associated with defective RAD6-dependent PRR (error-free bypass) of UV-damaged DNA (65). Furthermore, bulky lesions that block DNA synthesis on single-stranded template were bypassed *in vitro* when placed in fork-like DNA and incubated with extracts from HeLa or Chinese hamster ovary cells (66).

An alternative mechanism calls for the extension of the blocked leading strand after annealing of its 3′ end to the newly synthesized lagging strand that is identical in sequence and polarity to the damaged template. Such a template-switching mechanism, originally proposed by Higgins *et al.* (67) and Fugiwara and Tatsumi (68), could represent a caffeine-resistant pathway of PRR (31, 32, 68). Evidence supporting the uncoupling of leading and lagging strand synthesis (25, 56, 57, this report) and the possibility that the newly synthesized lagging strand could be extended by more than 1000 nucleotides beyond the dimer give new credence to the template-switching pathway. Furthermore, it is expected that copying of the undamaged lagging strand could be done at a much higher degree of fidelity than carrying out trans-lesion synthesis. Inactivation of this pathway may explain the XPV's defect in PRR (8, 31, 34), UV hypermutability (39–43), abnormal sensitivity to caffeine (31, 32, 68), and the deficiency in replication fork bypass described here.

In conclusion, our findings and those reported by others suggest that the XPV phenotype is related to the loss (or alteration) of a gene product that facilitates the relatively fast bypass of the pyrimidine dimer, perhaps through a template-switching mechanism or another error-free mechanism of bypass replication of pyrimidine dimers. However, if this gene product is a normal component of the DNA replication machinery, the XPV mutation does not appear to interfere with the replication of undamaged DNA. Finally, we suspect that the absence of a relatively fast mechanism for dimer bypass by replication forks leads to a prolonged arrest of replication at the photoproduct in XPV, interference with the removal of these DNA lesions by NER, and an increase in the probability of structural modifications of the dimer, such as deamination of cytosines (69, 70). When the replication machinery eventually overcomes the block, the ensuing trans-lesion synthesis, as the only option for bypass replication in XPV, would be associated with a high probability of base-substitution mutations.

Acknowledgments—This work was made possible by the generous contributions of Dr. Aziz Sancar (Dept. of Biochemistry and Biophysics, University of North Carolina, Chapel Hill), who provided the oligonucleotide containing the T[c,s]T dimer. We are grateful to Drs. Thomas A. Kunkel (NIEHS) and past members of his laboratory (Drs. John D. Roberts and David C. Thomas) for the gift of M13mp2SV and initial guidance with the *in vitro* replication assay. Drs. Sancar and Kunkel also offered valuable suggestions and constructive criticism during the

preparation of this manuscript. We thank Dr. J. W. Shay, University of Texas Southwestern Medical Center, Dr. Betsy Sutherland, Brookhaven National Institute, and Dr. James E. Cleaver, University of California at San Francisco, for the gifts of IDH4, SV80 and XP30RO/9.8 cell lines, respectively. T4 endonuclease V was kindly supplied by Dr. Isabel Mellon (University of Kentucky) and Dr. Stephen Lloyd (University of Texas Medical Branch at Galveston). We also acknowledge the help received from Dr. Jayne C. Boyer and Shyra J. Crider-Miller with some of the preliminary experiments.

REFERENCES

1. Scotto, J., Fears, T. R., and Fraumeni J. F., Jr. (1983) *Incidence of Nonmelanoma Skin Cancer in the United States*, NIH Publication No. 83-2433, pp. 1–14, National Cancer Institute, Bethesda, MD
2. Ananthaswamy, H. N., and Pierceall, W. E. (1990) *Photochem. Photobiol.* **52,** 1119–1136
3. Clingen, P. H., Arlett, C. F., Roza, L., Mori, T., Nikaido, O., and Green, M. H. L. (1995) *Cancer Res.* **55,** 2245–2248
4. International Agency for Research on Cancer Working Group (1992) *IARC Monogr. Eval. Carcinog. Risks Hum.* **55,** 43–279
5. Watanabe, M., Maher, V. M., and McCormick, J. J. (1985) *Mutat. Res.* **146,** 285–294
6. Kaufmann, W. K., and Wilson, S. J. (1994) *Mutat. Res.* **314,** 67–76
7. Kaufmann, W. K., and Cleaver, J. E. (1981) *J. Mol. Biol.* **149,** 171–187
8. Boyer, J. C., Kaufmann, W. K., Brylawski, B. P., and Cordeiro-Stone, M. (1990) *Cancer Res.* **50,** 2593–2598
9. Edenberg, H. J. (1976) *Biophys. J.* **16,** 849–860
10. Meneghini, R. (1976) *Biochim. Biophys. Acta* **425,** 419–427
11. Meneghini, R., and Hanawalt, P. (1976) *Biochim. Biophys. Acta* **425,** 428–437
12. Moore, P., and Strauss, B. S. (1979) *Nature* **278,** 664–666
13. Moore, P. D., Bose, K. K., Rabkin, S. D., and Strauss, B. S. (1981) *Proc. Natl. Acad. Sci. U. S. A.* **78,** 110–114
14. O'Day, C. L., Burgers, P. M. J., and Taylor, J.-S. (1992) *Nucleic Acids Res.* **20,** 5403–5406
15. Nelson, J. R., Lawrence, C. W., and Hinckle, D. C. (1996) *Science* **272,** 1646–1649
16. Ziegler, A., Leffell, D. J., Kunala, S., Sharma, H. W., Gailani, M., Simon, J. A., Halperin, A. J., Baden, H. P., Shapiro, P. E., Bale, A. E., and Brash, D. E. (1993) *Proc. Natl. Acad. Sci. U. S. A.* **90,** 4216–4220
17. Ziegler, A., Jonason, A. S., Leffell, D. J., Simon, J. A., Sharma, H. W., Kimmelman, J., Remington, L., Jacks, T., and Brash, D. E. (1994) *Nature* **372,** 773–776
18. Dumaz, N., Stary, A., Soussi, T., Daya-Grosjean, L., and Sarasin, A. (1994) *Mutat. Res.* **307,** 375–386
19. McGregor, W. G., Chen, R.-H., Lukash, L., Maher, V. M., and McCormick, J. J. (1991) *Mol. Cell. Biol.* **11,** 1927–1934
20. Bredberg, A., Kraemer, K. H., and Seidman, M. M. (1986) *Proc. Natl. Acad. Sci. U. S. A.* **83,** 8273–8277
21. Lebkowski, J. S., Clancy, S., Miller, J. H., and Calos, M. P. (1985) *Proc. Natl. Acad. Sci. U. S. A.* **82,** 8606–8610
22. Brash, D. E., Seetharam, S., Kraemer, K. H., Seidman, M. M., and Bredberg, A. (1987) *Proc. Natl. Acad. Sci. U. S. A.* **84,** 3782–3786
23. Carty, M. P., Hauser, J., Levine, A. S., and Dixon, K. (1993) *Mol. Cell. Biol.* **13,** 533–542
24. Thomas, D. C., and Kunkel, T. A. (1993) *Proc. Natl. Acad. Sci. U. S. A.* **90,** 7744–7748
25. Svoboda, D. L., and Vos, J.-M. H. (1995) *Proc. Natl. Acad. Sci. U. S. A.* **92,** 11975–11979
26. Carty, M. P., Lawrence, C. W., and Dixon, K. (1996) *J. Biol. Chem.* **271,** 9637–9647
27. Jung, E. G. (1970) *Nature* **228,** 361–362
28. Burk, P. G., Lutzner, M. A., Clarke, D. D., and Robbins, J. H. (1971) *J. Lab. Clin. Med.* **77,** 759–767
29. Cleaver, J. E. (1972) *J. Invest. Dermatol.* **58,** 124–128
30. Cleaver, J. E., Arutyunyan, R. M., Sarkisian, T., Kaufmann, W. K., Greene, A. E., and Coriell, L. (1980) *Carcinogenesis* **1,** 647–655
31. Lehmann, A. R., Kirk-Bell, S., Arlett, C. F., Paterson, M. C., Lohman, P. H. M., de Weerd-Kastelein, E. A., and Bootsma, D. (1975) *Proc. Natl. Acad. Sci. U. S. A.* **72,** 219–223
32. Cleaver, J. E., Thomas, G. H., and Park, S. D. (1979) *Biochim. Biophys. Acta* **564,** 122–131
33. Hessel, A., Siegle, R. J., Mitchell, D. L., and Cleaver, J. E. (1992) *Arch. Dermatol.* **128,** 1233–1237
34. van Zeeland, A. A., and Filon, A. R. (1982) *Prog. Mutat. Res.* **4,** 375–384
35. Thielmann, H. W., Popanda, O., Edler, L., and Jung, E. G. (1991) *Cancer Res.* **51,** 3456–3470
36. Cleaver, J. E., and Kraemer, K. H. (1995) in *The Metabolic and Molecular Bases of Inherited Disease* (Scriver, C. R., Beaudet, A. L., Sly, W. S., Valle, D., eds) Vol. 3, pp. 4393–4419, McGraw Hill Inc., New York
37. McCormick, J. J., Kateley-Kohler, S., Watanabe, M., and Maher, V. M. (1986) *Cancer Res.* **46,** 489–492
38. Boyer, J. C., Kaufmann, W. K., and Cordeiro-Stone, M. (1991) *Cancer Res.* **51,** 2960–2964
39. Maher, V. M., Ouellette, L. M., Curren, R. D., and McCormick, J. J. (1976) *Nature* **261,** 593–595
40. Myhr, B. C., Turnbull, D., and DiPaolo, J. A. (1979) *Mutat. Res.* **62,** 341–353
41. Wang, Y.-C., Maher, V. M., Mitchell, D. L., and McCormick, J. J. (1993) *Mol. Cell. Biol.* **13,** 4276–4283
42. Waters, H. L., Seetharam, S., Seidman, M. M., and Kraemer, K. H. (1993) *J. Invest. Dermatol* **101,** 744–748
43. Raha, M., Wang, G., Seidman, M. M., and Glazer, P. M. (1996) *Proc. Natl. Acad. Sci. U. S. A.* **93,** 2941–2946
44. King, S. A., Wilson, S. J., Farber, R. A., Kaufmann, W. K., and Cordeiro-Stone, M. (1995) *Exp. Cell Res.* **217,** 100–108
45. Volpe, J. P. G., and Cleaver, J. E. (1995) *Mutat. Res.* **337,** 111–117
46. Choi, K.-H., Tevethia, S. S., and Shin, S. (1983) *Cytogenet. Cell Genet.* **36,** 633–640
47. Shay, J. W., West, M. D., and Wright, W. E. (1992) *Exp. Gerontol.* **27,** 477–492
48. Li, J. J., and Kelly, T. J. (1984) *Proc. Natl. Acad. Sci. U. S. A.* **81,** 6973–6977
49. Roberts, J. D., and Kunkel, T. A. (1993) *Methods Mol. Genet.* **2,** 295–313
50. Roberts, J. D., and Kunkel, T. A. (1988) *Proc. Natl. Acad. Sci. U. S. A.* **85,** 7064–7068
51. Kunkel, T. A., Bebenek, K., and McClary, J. (1991) *Methods Enzymol.* **204,** 125–139
52. Huang, J.-C., Svoboda, D. L., Reardon, J. T., and Sancar, A. (1992) *Proc. Natl. Acad. Sci. U. S. A.* **89,** 3664–3668
53. Brewer, B. J., and Fangman, W. L. (1987) *Cell* **51,** 463–471
54. Brewer, B. J., Sena, E. P., and Fangman, W. L. (1988) *Cancer Cells* **6,** 229–234
55. Li, J. J., and Kelly, T. J. (1985) *Mol. Cell. Biol.* **5,** 1238–1246
56. Thomas, D. C., Veaute, X., Kunkel, T. A., and Fuchs, R. P. P. (1994) *Proc. Natl. Acad. Sci. U. S. A.* **91,** 7752–7756
57. Thomas, D. C., Veaute, X., Fuchs, R. P. P., and Kunkel, T. A. (1995) *J. Biol. Chem.* **270,** 21226–21233
58. Lehman, A. R. (1972) *J. Mol. Biol.* **66,** 319–337
59. Meneghini, R., Cordeiro-Stone, M., and Schumacher, R. I. (1981) *Biophys. J.* **33,** 81–92
60. Kaufmann, W. K. (1989) *Carcinogenesis* **10,** 1–11
61. Cordeiro-Stone, M., Schumacher, R. I., and Meneghini, R. (1979) *Biophys. J.* **27,** 287–300
62. Little, R. D., Platt, T. H. K., and Schildkraut, C. L. (1993) *Mol. Cell. Biol.* **13,** 6600–6613
63. Dijkwel, P. A., Vaughn, J. P., and Hamlin, J. L. (1994) *Nucleic Acids Res.* **22,** 4989–4996
64. Waga, S., and Stillman, B. (1994) *Nature* **369,** 207–212
65. Torres-Ramos, C. A., Yoder, B. L., Burgers, P. M. J., Prakash, S., and Prakash, L. (1996) *Proc. Natl. Acad. Sci. U. S. A.* **93,** 9676–9681
66. Hoffmann, J.-S., Pillaire, M.-J., Lesca, C., Burnouf, D., Fuchs, R. P. P., Defais, M., and Villani, G. (1996) *Proc. Natl. Acad. Sci. U. S. A.* **93,** 13766–13769
67. Higgins, N. P., Kato, K., and Strauss, B. (1976) *J. Mol. Biol.* **101,** 417–425
68. Fugiwara, Y., and Tatsumi, M. (1976) *Mutat. Res.* **37,** 91–110
69. Setlow, R. B., Carrier, W. L., and Bollum, F. J. (1965) *Proc. Natl. Acad. Sci. U. S. A.* **53,** 1111–1118
70. Tessman, I., Liu, S.-K., and Kennedy, M. A. (1992) *Proc. Natl. Acad. Sci. U. S. A.* **89,** 1159–1163